Potential vorticity in warm conveyor belt outflow

Methven, J. (2015) Potential vorticity in warm conveyor belt outflow. Quarterly Journal of the Royal Meteorological Society, 141 (689). pp. 1065-1071. ISSN 0035-9009 doi: https://doi.org/10.1002/qj.2393 Available at https://centaur.reading.ac.uk/39384/

RMetS
Royal Meteorological Society

Potential vorticity in warm conveyor belt outflow

John Methven*
Department of Meteorology, University of Reading, UK

*Correspondence to: J. Methven, Department of Meteorology, University of Reading, Earley Gate, Reading, RG6 6BB, UK.
E-mail: j.methven@reading.ac.uk

Warm conveyor belts (WCBs) are the main ascending air masses within extratropical cyclones. They often exhibit strong condensation and precipitation, associated with ascent on large scales or embedded convection. Most of the air outflows into the upper troposphere as part of a ridge. Such ridges are an integral part of Rossby waves propagating along the tropopause and are identified with a negative potential vorticity (PV) anomaly and associated anticyclonic circulation. It has been argued that diabatic modification of PV in WCBs has an important influence on the extent of the ridge, propagation of Rossby waves and weather impacts downstream.

Following the coherent ensemble of trajectories defining a WCB, PV is expected to increase with time while below the level of maximum latent heating and then decrease as trajectories ascend above the heating maximum. In models, it is found that the net change is approximately zero, so that the average PV of the WCB outflow is almost equal to the PV of its inflow. Here, the conditions necessary for this evolution are explored analytically using constraints arising from the conservation of circulation. It is argued that the net PV change is insensitive to the details of diabatic processes and the PV maximum midway along a WCB depends primarily on the net diabatic transport of mass from the inflow to the outflow layer. The main effect of diabatic processes within a WCB is to raise the isentropic level of the outflow, rather than to modify PV.

Key Words: circulation; conservation; diabatic transport; Rossby waves

Received 25 July 2013; Revised 22 April 2014; Accepted 6 May 2014; Published online in Wiley Online Library

1. Introduction

Warm conveyor belts (WCBs) are ascending air masses in the warm sector of an extratropical cyclone (Browning, 1971; Harrold, 1973). The horizontal component of the trajectories is almost parallel to the cold front, either running on the warm side of the surface cold front or riding up the frontal surface in the case of ana-cold fronts. Wernli and Davies (1997) identified WCBs with a coherent ensemble of trajectories, usually selected from a much greater set of trajectories by meeting a criterion based on net ascent (for example, a pressure decrease exceeding 600 hPa). The outflow of warm conveyor belts can split into two branches: one turns cyclonically around the poleward flank of the cyclone centre, while the other turns anticylonically into the large-scale ridge, as depicted in figure 1 of Thorncroft *et al.* (1993). Typically the anticyclonic branch is higher, forming a lens of air that spreads across the ridge just below the tropopause (Browning and Roberts, 1994; Martinez-Alvarado *et al.*, 2013). The ridge itself is not static and develops as the poleward-moving WCB air enters it.

In the ridge, the tropopause is higher than elsewhere at the same latitude and is therefore associated with a negative potential vorticity (PV) anomaly. It forms an integral part of the PV pattern at tropopause level that propagates via the Rossby-wave mechanism. Davies and Didone (2013) have studied the PV errors of a forecast and argue that 'despite the complexity of cloud processes, the net PV change may not be large. Nevertheless the mere deposition of lower-tropospheric air with low PV at tropopause levels would be dynamically significant because it would constitute a major negative PV anomaly relative to its surroundings.' Pomroy and Thorpe (2000) argued that diabatic processes in the WCB exert an influence on the PV of the outflow and therefore on the downstream propagation of Rossby waves. They used a reverse domain-filling trajectory technique to identify the net change in PV along trajectories obtained by interpolating the Met Office forecast model output to trajectory points. They showed in two case studies that the PV on trajectories identified with the WCB is lower in the outflow than at the inflow points, although this must depend on the length of back trajectories chosen (discussed again in the Conclusions). The net PV change was associated with a 'diabatic PV anomaly' and then inverted to determine the anticyclonic flow induced by it. A re-run of the model from initial conditions with the negative diabatic PV anomaly subtracted is similar, but the difference from the original run reflects the signature of the

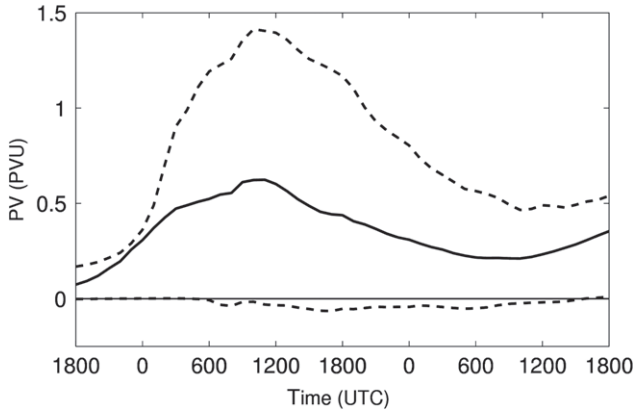

Figure 1. Potential vorticity evolution following a warm conveyor belt defined by a coherent ensemble of trajectories in a simulation using the Met Office Unified Model by Martinez-Alvarado *et al.* (2013). The bold line shows the ensemble mean and dashed lines show the 15th and 85th percentile of PV values across the ensemble.

change to Rossby-wave propagation along the jet. More recently, Joos and Wernli (2012) have presented results where the net PV change along a WCB trajectory ensemble is also negative, but the PV changes are calculated from the heating associated with microphysical processes in the Consortium for Small-Scale Modelling (COSMO) numerical weather prediction (NWP) model, rather than obtaining net changes by interpolation.

In contrast, Martinez-Alvarado *et al.* (2013) have presented a case study using two different NWP models (the Met Office Unified Model and COSMO) where there was a small net increase in PV along WCB trajectories. Figure 1 shows the evolution of PV from the Met Office model following a coherent ensemble of trajectories (CET) in terms of the ensemble mean and the 15th and 85th percentiles. There is a clear maximum in ensemble-average PV midway through the ascent. This CET forms the anticyclonic branch of a WCB. At any one time, the envelope of trajectory points defines a volume. The inflow volume (initial time in Figure 1) was located at a mean pressure of 980 hPa (with an interquartile range of 50 hPa) and the trajectories ascended to a mean outflow pressure of 325 hPa (interquartile range 60 hPa), which was near the tropopause in the downstream ridge. In isentropic coordinates, the ensemble-mean position (and θ range) of the inflow volume was at a potential temperature of 289 K (3 K), increasing through heating to the outflow volume at 318 K (7 K). Madonna *et al.* (2014) present a climatology of WCBs identified with CETs meeting the criterion of 600 hPa ascent within 48 h, as calculated from the ERA-Interim dataset. Their figure 6 shows the composite time evolution for the North Atlantic region, taking all events in winter (DJF) from 1979–2010. The PV evolution and potential temperature increase is very similar to the case shown in Figure 1.

The evidence is that PV increases in the lower troposphere and then decreases such that the net PV change is near zero following trajectories through a WCB. This article seeks to explain this behaviour theoretically and addresses the question of how diabatic processes, including latent heat release and diabatic mixing, might influence WCB outflow by constructing a simple thought experiment and analyzing the evolution of PV. Section 2 recalls some results concerning PV conservation and section 3 considers the implications for the evolution along WCBs. Section 4 discusses the possible influences of motions that are unresolved (subgrid-scale) in the models used to calculate the trajectories. Conclusions are presented in section 5.

2. PV conservation

For adiabatic and frictionless flow without mixing, both potential temperature (θ) and Ertel PV (q) are materially conserved, meaning that their values do not change following air parcels. Therefore, it is useful to use θ as a vertical coordinate because, in the absence of heating, air parcel trajectories will be constrained to follow isentropic levels (surfaces of constant θ). Diabatic processes are therefore necessary to enable vertical motion in isentropic coordinates. Pseudo-density in isentropic coordinates is defined by considering the small mass element

$$\mathrm{d}m = \rho \,\mathrm{d}A\,\mathrm{d}z = r\,\mathrm{d}A\,\mathrm{d}\theta, \tag{1}$$

where ρ is the air density, r is the pseudo-density and $\mathrm{d}A$ is an area element on the appropriate level surface. The mass continuity equation in isentropic coordinates is then

$$\frac{\partial r}{\partial t} + \nabla.\,(r\mathbf{V}) + \frac{\partial}{\partial \theta}\left(r\dot{\theta}\right) = 0, \tag{2}$$

where $\mathbf{V} = (u, v, 0)$ is the horizontal velocity along isentropic surfaces and $\dot{\theta}$ is the heating rate or vertical velocity in isentropic coordinates. Under the approximations of the hydrostatic primitive equations, the pseudo-density is given by $r = -(1/g)\partial p/\partial\theta$ and Ertel PV takes the simple form $q = \zeta/r$, where ζ is the vertical component of absolute vorticity evaluated by taking derivatives of the horizontal velocity components along isentropic surfaces. Haynes and McIntyre (1987) derived the equation for the conservation of Ertel PV, q, in a flux form:

$$\frac{\partial}{\partial t}\left(rq\right) + \nabla.\left(rq\mathbf{V}\right) + \nabla.\mathbf{J} = 0, \tag{3}$$

where the hydrostatic, isentropic coordinate expression for the non-advective PV flux is

$$\mathbf{J} = \left(\dot{\theta}\frac{\partial v}{\partial\theta} - F_y, -\dot{\theta}\frac{\partial u}{\partial\theta} + F_x, 0\right), \tag{4}$$

where F_x and F_y represent the horizontal components of forces acting on fluid parcels (typically from viscous stresses). $\mathbf{J}$ has no vertical component (across isentropic surfaces). Haynes and McIntyre (1990) use this result to describe isentropic surfaces as 'impermeable to PV substance'. If the PV, q, is associated with the notional mass mixing ratio of a trace constituent called 'PV substance', then the lack of vertical component in $\mathbf{J}$ implies that there is no cross-isentropic flux of PV substance. Haynes and McIntyre (1987) also showed that Eq. (3) and the impermeability theorem are valid for non-hydrostatic flow, where the 3-D velocity $\mathbf{u}$ appears in the advective flux, and the general non-advective flux vector $\mathbf{J} = -\dot{\theta}\boldsymbol{\zeta} - \mathbf{F}\times\nabla\theta$, where $\boldsymbol{\zeta}$ is the absolute vorticity vector and $\mathbf{F}$ represents friction or an arbitrary force per unit mass.

In contrast, a trace constituent with mass mixing ratio χ will obey the continuity equation,

$$\frac{\partial}{\partial t}(r\chi) + \nabla.\,(r\chi\mathbf{V}) + \frac{\partial}{\partial\theta}\left(r\chi\dot{\theta}\right) = rS, \tag{5}$$

which has a vertical flux associated with $\dot{\theta}$. S represents a material source or sink of tracer (per unit mass of air).

Here, the impermeability result will be used to analyze changes in PV along a warm conveyor belt. First, integrate mass continuity Eq. (2) over a volume sandwiched between two isentropic surfaces separated by a fixed distance $\Delta\theta$:

$$\begin{aligned}\frac{\mathrm{d}}{\mathrm{d}t}\iiint r\,\mathrm{d}A\,\mathrm{d}\theta + \oiint r\left(\mathbf{V}-\mathbf{V}_\mathrm{b}\right).\mathbf{n}\,\mathrm{d}l\,\mathrm{d}\theta \\ + \iint\left[r\dot{\theta}\right]_{\mathrm{bot}}^{\mathrm{top}}\mathrm{d}A = 0, \\ \frac{\mathrm{d}M}{\mathrm{d}t} = -D_{\mathrm{top}} + D_{\mathrm{bot}}.\end{aligned} \tag{6}$$

The first equation above is derived using Gauss' theorem and the Leibnitz formula for differentiation: the time rate of

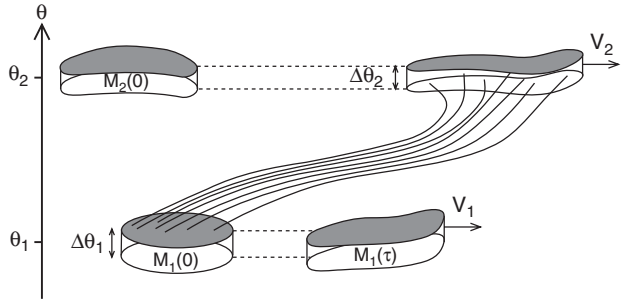

Figure 2. Schematic of the control volumes in the thought experiment (see text). Volume 1 encompasses the warm conveyor belt inflow at the initial time, centred on isentropic surface θ_1 with depth $\Delta\theta_1$ and initial mass $M_1(0)$. The lateral boundary of volume 1 follows the horizontal flow within its isentropic layer, $\mathbf{V}_1$, and loses mass through diabatic transport out of its top face, resulting in mass $M_1(\tau)$ by time $t = \tau$. The coherent ensemble of trajectories (CET) depicts the mass transport in the warm conveyor belt crossing from layer 1 to the higher outflow layer (centred on θ_2). The CET envelope forms a material volume following the resolved 3-D flow. Volume 2 is defined such that it encompasses the WCB outflow at $t = \tau$. This control volume can be traced backwards in time following the horizontal flow in isentropic layer 2, $\mathbf{V}_2$, to the initial time when it had mass $M_2(0)$. Note that in general $\mathbf{V}_2 \neq \mathbf{V}_1$. Typically the flow is stronger aloft and the layers are shallow relative to their separation ($\theta_2 - \theta_1$).

change of an integral (mass M) depends on the rate of change of its integrand (r) and the change in limits of integration if the boundary moves. Here, dl is a distance element around the closed circuit formed by the intersection of the volume's lateral boundary with each isentropic surface. **n** is the outward-pointing normal of the lateral boundary and $\mathbf{V}_\mathrm{b}$ is the velocity of the boundary along an isentropic surface. In the second equality, the lateral boundary is defined to move with the isentropic flow such that $\mathbf{V}_\mathrm{b} = \mathbf{V}$. M is the mass within the volume

$$M = \iiint r \,\mathrm{d}A \,\mathrm{d}\theta \tag{7}$$

and D is the upward diabatic mass flux across the top or bottom isentropic surface of the volume. Note that this is the same control volume as depicted in figure 1 of Haynes and McIntyre (1987) and in Figure 2 below. Integrating the PV equation (3) over the control volume gives

$$\begin{aligned} &\frac{\mathrm{d}}{\mathrm{d}t}\iiint rq \,\mathrm{d}A \,\mathrm{d}\theta \\ &\qquad + \oint\!\!\!\oint \left\{rq\left(\mathbf{V} - \mathbf{V}_\mathrm{b}\right) + \mathbf{J}\right\}.\mathbf{n} \,\mathrm{d}l \,\mathrm{d}\theta = 0, \\ &\frac{\mathrm{d}}{\mathrm{d}t}\left(C\Delta\theta\right) = \Delta\theta\frac{\mathrm{d}C}{\mathrm{d}t} = 0, \end{aligned} \tag{8}$$

where we have also defined the control volume such that **J.n** integrates to zero around its lateral boundary (to be justified below) and C is the circulation around the boundary, averaged over the fixed depth of the volume $\Delta\theta$:

$$C\Delta\theta = \iiint rq \,\mathrm{d}A \,\mathrm{d}\theta = \oint\!\!\!\oint \mathbf{V}_\mathrm{abs}.\mathbf{s} \,\mathrm{d}l \,\mathrm{d}\theta. \tag{9}$$

The last step uses Stokes' theorem and the fact that rq is the vertical component of absolute vorticity and **s** is a unit vector along an isentropic surface, parallel to the boundary. Equation (8) is simply a statement of Kelvin's circulation theorem valid in the special circumstance **J.n** integrates to zero around the lateral boundary (although heating can be non-zero within the volume and mass can be transported in or out diabatically). Note that no assumptions have been made regarding the shape of the control volume. It can be assumed that $\mathbf{J} = 0$ is achieved through negligible heating or friction on the lateral boundary, rather than a restriction on the vertical wind shear in Eq. (4).

3. PV changes following a warm conveyor belt

3.1. Definition of control volumes

The aim is to calculate the average change in PV through a warm conveyor belt from its inflow into the outflow. Following Wernli and Davies (1997) define a WCB as a material volume described by a coherent ensemble of 3-D trajectories (CET) that ascends and experiences heating such that θ increases. The PV conservation Eq. (3) can be written in its Lagrangian (hydrostatic) form:

$$r\frac{\mathrm{D}q}{\mathrm{D}t} = \frac{\partial\left(rq\dot{\theta}\right)}{\partial\theta} - \nabla.\mathbf{J}, \tag{10}$$

where $\mathrm{D}q/\mathrm{D}t$ denotes the rate of change in PV following a 3-D trajectory. Haynes and McIntyre (1987) argue that under quasi-geostrophic scaling (with weak friction), the first term on the right-hand side dominates. Therefore, following the trajectories of the WCB, increase in PV is expected below the heating maximum associated with latent heat release, followed by a decrease in PV moving out above the maximum. However, there is no obvious constraint on the value of PV that might emerge in the ouflow. The result would depend on the vertical profile of heating plus effects of the vertical wind shear in the $\nabla.\mathbf{J}$ term. The aim is to use the flux form of PV conservation and the PV impermeability theorem discussed in section 2 to consider constraints on the ensemble-average PV in the outflow of WCBs.

Define the mass-weighted average PV as

$$\langle q\rangle = \frac{\iiint rq \,\mathrm{d}A \,\mathrm{d}\theta}{\iiint r \,\mathrm{d}A \,\mathrm{d}\theta} = \frac{C\Delta\theta}{M}. \tag{11}$$

Now, consider two control volumes, as illustrated in Figure 2. Volume 1 (the inflow volume) encompasses the CET just before ascent begins and is sandwiched in an isentropic layer of depth $\Delta\theta_1$ with midlayer position θ_1. Volume 2 (the outflow volume) contains the CET at a later time τ when ascent has finished (with depth $\Delta\theta_2$ at position θ_2). As discussed in section 1, it is typically found that the net diabatic motion $\theta_2 - \theta_1$ is considerably greater than the inflow or outflow layer depths, $\Delta\theta_1$ and $\Delta\theta_2$.

Typically, the trajectories defining a WCB represented by a numerical weather prediction model are calculated following the flow resolved by the model. A CET calculated in this way defines a material volume in the sense that the mass contained within it does not exchange with its surroundings following the resolved flow. Therefore, its mass is invariant. Since volume 2 is connected to volume 1 by the WCB, it is natural to define the mass of volume 2 at $t = \tau$ to equal the initial mass of volume 1:

$$M_2(\tau) = M_1(0) = M_0. \tag{12}$$

It then follows trivially that the average PV of volume 1 at the initial time and volume 2 at the final time are

$$\langle q\rangle_1(0) = \frac{C_1\Delta\theta_1}{M_0}; \qquad \langle q\rangle_2(\tau) = \frac{C_2\Delta\theta_2}{M_0}. \tag{13}$$

3.2. Evolution of PV in control volumes

Properties of volumes encompassing the start and end points of the WCB have been defined, but nothing has yet been deduced about the evolution between these two time points. However, Eq. (8) states that circulation is conserved, even when diabatic processes are acting, if we consider control volumes confined within isentropic layers with lateral boundaries following the flow along isentropic surfaces. This motivates consideration of two such control volumes distinct from the CET itself: volume 1 confined to the layer $\theta_1 - \Delta\theta_1/2 < \theta < \theta_1 + \Delta\theta_1/2$ with invariant circulation $C_1\Delta\theta_1$ and volume 2 confined to the layer $\theta_2 - \Delta\theta_2/2 < \theta < \theta_2 + \Delta\theta_2/2$ with invariant circulation $C_2\Delta\theta_2$.

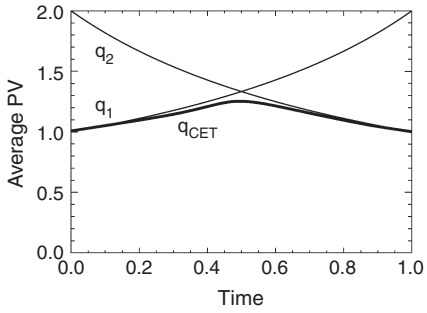

Figure 3. The evolution of the average PV in the inflow and outflow control volumes, labelled 1 and 2, as given by Eq. (15) in a simple scenario (see text). At the initial time, volume 1 (inflow) contains the coherent ensemble of trajectories defining the WCB. Volume 2 (outflow) is defined to contain the CET at the final time ($t/\tau = 1$). The key assumption is that all the mass transported diabatically out of volume 1 eventually enters volume 2 by $t = \tau$. Since the volume defined by the CET (which follows the resolved 3-D flow) is initially near the inflow and at later times reaches the level of the outflow, the average PV of the CET can be approximated by the bold curve, which has a maximum during the interval.

Each control volume is not a material volume, since it is constrained to follow the flow in one layer and diabatic processes can transport mass across the bottom or top isentropic surface of the layer. The lateral boundary is assumed to surround the isolated region of latent heat release associated with the WCB at that level and to lie outside it, so that **J**.**n** integrates to zero around the lateral boundary as assumed for Eq. (8). The lower surface of volume 1 is assumed to be below the level of condensation where $\dot{\theta} = 0$ so that $D_{1,\mathrm{bot}} = 0$, while on the upper surface in general there is heating within the bounding circuit. As a result of heating on the top surface, we expect a diabatic mass flux out of volume 1 and for its mass to decrease (recall that there is no mass flux across the lateral boundary, because it moves with the horizontal fluid velocity).

Similarly, volume 2 remains confined in the isentropic layer 2 with a lateral boundary following the isentropic flow in that layer. Now let us assume that all the mass transported diabatically out of volume 1, ΔM, follows the CET and is deposited through diabatic transport into the outflow volume by time $t = \tau$. It is also assumed that there is no diabatic transport across the top of volume 2, $D_{2,\mathrm{top}} = 0$. Then it is the case that

$$M_1(\tau) = M_1(0) - \Delta M; \qquad M_2(\tau) = M_2(0) + \Delta M. \quad (14)$$

Although circulation is invariant for each control volume, their mass-weighted average PV can change as a result of varying mass. An expression for the evolution of PV in each control volume is sought. Now define the diabatic mass transport from volume 1 by the time-dependent function, $m_1(t)$, which increases from 0 to ΔM, and the deposition of mass into volume 2 by $m_2(t)$, which also increases from 0 to ΔM. In general, there is a gap between $\theta_1 + \Delta\theta_1/2$ and $\theta_2 - \Delta\theta_2/2$ (as depicted in Figure 2), so the increase in m_2 will lag m_1. Then, in the interval $0 < t < \tau$,

$$\langle q \rangle_1 (t) = \frac{C_1 \Delta\theta_1}{M_0} \left(\frac{1}{1 - \frac{m_1(t)}{M_0}} \right), \quad (15)$$

$$\langle q \rangle_2 (t) = \frac{C_2 \Delta\theta_2}{M_0} \left(\frac{1}{1 + \frac{m_2(t) - \Delta M}{M_0}} \right).$$

Figure 3 depicts a simple symmetric example where the diabatic mass transport is linear in time and is immediately transferred from volume 1 to volume 2 ($m_2 = m_1 = \Delta M\, t/\tau$), half the mass is eventually transported out of the inflow layer ($\Delta M/M_0 = 0.5$) and the circulations of the two layers are equal ($C_1\Delta\theta_1 = C_2\Delta\theta_2$). The PV increases in volume 1 as a result of diabatic mass transport from it and concentration of PV substance. The PV decreases in volume 2 due to dilution of PV substance by the diabatic mass influx.

Equation (15) does not give the evolution of PV following the CET material volume. However, by definition, at $t = 0$ the CET is a subset of volume 1 and at $t = \tau$ it is a subset of volume 2. As already argued below Eq. (10), the PV is expected to increase while below the level of maximum heating along the WCB and decrease again above it. The bold curve is a qualitative indication of the evolution of average PV following the CET as it traverses from volume 1 to volume 2. Note that the variation in q_{CET} is small compared with the NWP model result in Figure 1. However, if the inflow and outflow isentropic layers are well separated, as in Figure 2, then one can expect a delay between mass leaving volume 1 and arriving in volume 2. This would enable average PV to increase in the inflow layer before it decreases in the outflow layer, contributing to a greater maximum in PV midway following the CET. Nevertheless, the mass-weighted integral of PV substance in volume 2 cannot change, since it equals $C_2\Delta\theta_2$, which is invariant (Eq. (8)). The temporal maximum of ensemble-average PV for the CET is given approximately at the time when the PV values of the two control volumes are equal (the curves cross in Figure 3). From Eq. (15), the PV values can cross when the ratio of circulations of the two volumes lies within the range

$$\left(1 - \frac{\Delta M}{M_0}\right) < \frac{C_2\Delta\theta_2}{C_1\Delta\theta_1} < \left(1 - \frac{\Delta M}{M_0}\right)^{-1} \quad (16)$$

and therefore a PV maximum is expected for cases within this range.

3.3. *The limit of weak heating*

In the adiabatic limit, there is no diabatic mass transport ($\Delta M = 0$ and $\theta_2 - \theta_1 = 0$) and volumes 1 and 2 are equal at all times. Therefore, their masses and circulations must also be identical and time-invariant (i.e. they are material volumes for adiabatic flow).

Now consider a special situation with weak net heating where the outflow layer is higher than the inflow, but the two layers just touch (i.e. $\theta_2 - \Delta\theta_2/2 = \theta_1 + \Delta\theta_1/2$). The circulations of the two volumes will be similar if the layers are shallow (depth h) relative to the depth-scale of the flow in the baroclinic wave containing the WCB. Assuming that the depth-scale of horizontal velocity takes the usual quasi-geostrophic scaling $H \sim fL/N$, this requires that $Nh/(fL) \ll 1$. The vertical wind shear is weak across volumes that are shallow in this sense, helping to support the supposition that the non-advective PV flux $\mathbf{J} \approx 0$, from Eq. (4). In this scenario, $C_2\Delta\theta_2 \approx C_1\Delta\theta_1$ and, from Eq. (13), the average PV of the CET outflow (at $t = \tau$) is expected to equal approximately the initial average PV of the inflow.

In realistic cases, heating is stronger and the separation of the outflow from the inflow is much greater than the depth of either the volume, h, or the depth-scale of horizontal velocity, H. The inflow occurs within, or just above, the boundary layer and the outflow of a WCB enters a thin layer just below the tropopause. For example, in the climatology of Madonna *et al.* (2014), the composite WCB evolution for North Atlantic winter yields the parameters $\Delta\theta_1 = 6\,\mathrm{K}$ and $\Delta\theta_2 = 12\,\mathrm{K}$, while $\theta_1 = 292\,\mathrm{K}$ and $\theta_2 = 315\,\mathrm{K}$, giving $\theta_2 - \theta_1 = 23\,\mathrm{K}$. The case study of Martinez-Alvarado *et al.* (2013) indicated a greater net θ increase and even tighter spread on the inflow and outflow layers (numbers given in section 1). In this scenario, it is reasonable to assume that both the inflow and outflow volumes (labelled 1 and 2) are shallow relative to the depth-scale of velocity (H) but there is strong shear between the two levels, as depicted in Figure 2. In this case, although Eq. (13) must hold, there is no reason to expect *a priori* that the PV of the outflow matches the PV of the inflow, since the volumes could encompass different amounts of PV substance ($C_2\Delta\theta_2 \neq C_1\Delta\theta_1$). However, the climatology of Madonna *et al.* (2014) shows that the average

PV of the outflow does approximately equal the PV of the inflow, indicating that a similar amount of PV substance must be enclosed within the inflow and outflow volumes associated with the coherent ensembles of trajectories that they calculate from re-analyses.

4. Effects of unresolved motions

The warm conveyor belt is a description that was originally conceived by Browning (1971) and Harrold (1973) to link the frontal structure in observed cold frontal zones with the large-scale flow in cyclones revealed by isentropic relative flow analysis performed using data from the synoptic-scale network. Subsequently, in the identification of WCBs, isentropic relative flow analysis was superceded by trajectory calculations using the 3-D flow from models or meteorological analyses. Following Wernli and Davies (1997), WCBs were defined by coherent ensembles of trajectories (CETs), identified by applying certain trajectory criteria such as net ascent. This concept was used to construct the thought experiment and Figure 2. Trajectories calculated using analyses have been shown to provide very accurate depictions of the structure within extratropical cyclones associated with the interleaving of air masses with different properties and origins (e.g. Methven *et al.*, 2003). However, WCBs are characterized by strong turbulence associated with clouds and embedded convection. These motions cannot be resolved by the model producing a global analysis, so it is necessary to consider what impact they could have on the conclusions drawn in the last section.

Sometimes the meaning of trajectories calculated following resolved winds from a model in a situation with strong subgrid-scale motion is questioned. Often the argument is given that the trajectories cannot follow the path of individual air parcels and therefore are not meaningful, or that a stochastic step representing subgrid-scale turbulence should be included. The thought experiment pictured in Figure 2 makes clear the robustness of the coherent trajectory ensemble view. The important aspect is the model-resolved adiabatic flow. In the thought experiment, control volumes 1 and 2 are constrained to remain within their initial isentropic layers. The movement and distortion of the lateral boundary of each volume is expected to be well represented by the resolved isentropic flow. Methven and Hoskins (1999) showed that tracer structures that are an order of magnitude smaller than the smallest retained scales in the wind field can be accurately represented in Lagrangian or tracer transport models. Fast vertical motions that are essentially adiabatic (such as undulating gravity waves) only result in the temporary vertical displacement of isentropic surfaces and have little effect on the horizontal stirring. Section 3 shows that the details of the cross-isentropic motion are also not important to PV, so long as the net diabatic transport of mass from control volume 1 to volume 2 is simulated well. The reason is that PV substance cannot cross between the isentropic layers even in the presence of diabatic or frictional effects. Only mass is transferred by diabatic transport.

The interpretation of 3-D trajectories following the resolved flow is that their isentropic component (including the effects of strain and vertical wind shear) traces the path of an air mass and their cross-isentropic component represents the integrated heating experienced. Martinez-Alvarado *et al.* (2013) have shown the similarity of WCB trajectories and their properties such as net ascent in simulations of the same case with two numerical weather prediction models that differ substantially in the representation of parametrized processes such as moist convection and turbulence. The net PV evolution is similar in both models following the CETs. However, it was shown that the net heating along CETs was sensitive to the convection scheme, which then influenced the mean WCB outflow level and the subsequent split between the cyclonic and anticyclonic branches of the WCB. Stronger heating enabled more trajectories to access higher θ levels and populate the anticyclonic branch.

Note that these conclusions do not carry over to trace constituents. Equation (5) makes clear that there will be vertical transport associated with correlations between tracer mixing ratio and heating at the top of the inflow volume. The tracer can pass through this boundary, while PV substance cannot. Therefore, we can expect that the redistribution of tracer by a WCB will have some dependence on the representation of vertical transport, including large-scale ascent, convection and small-scale turbulent mixing. For example, Agusti-Panareda *et al.* (2005) have shown, using a simulation of a summer WCB case across Europe, that tracer export from the boundary layer is approximately halved when mass fluxes from the convection parametrization are not included in the tracer transport calculation.

5. Conclusions and discussion

The defining characteristic of WCB transport lies in the net diabatic mass transport between two distinct isentropic layers and the horizontal component of the trajectories in isentropic coordinates. The details of the cross-isentropic component of the trajectories are not especially important to PV. A consequence is that we should expect the results for the WCB evolution to be similar from high-resolution convection-permitting models and lower resolution models with parametrized convection, provided that the parametrization yields similar results for the heating averaged along the WCB path.

In the thought experiment presented in section 3, three distinct control volumes were introduced. The first is the material volume described by a coherent ensemble of trajectories taken to define a warm conveyor belt. Although its mass is invariant, it is not straightforward to predict what would happen to the average PV (or circulation) of this volume in the presence of diabatic processes.

Therefore, two further control volumes are introduced. Volume 1 encompasses the CET volume at time $t = 0$ just before WCB ascent begins. Volume 2 encompasses the CET volume at time $t = \tau$ just after WCB ascent has finished. However, these volumes are constrained to remain within isentropic layers following the isentropic flow and are therefore not material volumes in the presence of diabatic processes, since mass can cross in or out of the layers where heating is present on their bounding isentropic surfaces. The reason to use these volumes is that, under certain assumptions, circulation is conserved following both volumes. This is a consequence of the impermeability theorem for PV. As argued by Haynes and McIntyre (1990), PV substance cannot be transported between isentropic layers, in contrast to the mixing ratio of chemical tracers. This property results in Eq. (15) describing the evolution of the average PV of each volume over the interval $0 < t < \tau$. The PV of volume 1 increases with time as mass is lost from it and PV substance concentrates, while the PV of volume 2 decreases with time as the mass entering dilutes PV substance there. It was shown that the average PV of the CET volume must increase to a maximum at some intermediate time and then decrease towards the average PV of the outflow volume at $t = \tau$.

The conservation of circulation, or mass-weighted integral PV, for both control volumes 1 and 2, implies that the circulation of the upper volume is not influenced by the lower volume. However, by construction the volumes are connected in terms of mass transport by the CET. Since the mass of the CET is invariant, it was chosen to specify the mass of volume 2 at $t = \tau$ such that it equals the mass of volume 1 at $t = 0$ (Eq. (12)). Taken together, it implies that the average PV of the outflow volume (at $t = \tau$) can only equal the average PV of the inflow (at $t = 0$) if they contain the same circulation at all times (Eq. (13)). One would expect these conditions to be met approximately in the special situation where the vertical separation of the inflow and outflow volumes is small relative to the depth-scale of horizontal flow. However, the WCBs in the climatology of Madonna *et al.* (2014) ascend throughout the depth of the troposphere (> 600 hPa

by definition) and yet satisfy $\langle q \rangle_2 (\tau) \approx \langle q \rangle_1 (0)$. Although the structure of poleward flow in WCBs can be untilted and can extend throughout the troposphere, it is typically the case that the depth-scale of horizontal motions is shallower than the depth of the troposphere and so a direct equality cannot be expected to hold generally.

The result is not dependent on the nature of heating or diabatic mixing throughout the WCB. There are only two assumptions. (1) All the mass leaving the inflow volume enters the outflow volume by time τ and there is no other diabatic mass transport across either volume. (2) The circuit integral of the non-advective PV flux **J** around the lateral boundaries of each volume is zero. This implies that there are no net frictional effects and the lateral boundaries of both control volumes can be moved to a location where the heating is zero, even though there is heating within the volumes and between them. There are no restrictions on the geometry of the two volumes and they could be separate, connecting or even overlapping. Only the maximum PV value attained following the WCB is influenced by the strength of heating, the net diabatic mass flux and the lag between the mass flux leaving the inflow volume and entering the outflow volume (see Figure 2).

The key processes that would violate the conditions for Eq. (15) are friction and heating acting on the lateral boundaries, heating on the lower isentropic face of the inflow volume or heating at the top of the outflow volume. Friction, or eddy viscosity, would act systematically to spin down the circulation. It would be expected to be strongest within the boundary layer and therefore act to decrease average PV in the inflow volume. Similarly, heating on the lower isentropic face of the inflow volume would result in diabatic transport of mass into the volume, diluting the average PV. A special situation occurs when the isentropic layer of the inflow volume intersects the ground–this is effectively a lateral boundary in isentropic coordinates. Where the vertical component of absolute vorticity is positive, surface heating would act to decrease the circulation. Hoskins (1991) has discussed the importance of friction and surface heating to the time-mean circulation about Antarctica and Tibet using similar arguments. Therefore, the expectation is that the systematic effect of these other processes would be to decrease the average PV of the inflow volume, with no direct influence on the outflow volume. Indeed, Chagnon *et al.* (2013) have observed using diabatic PV tracers that the boundary-layer scheme in the Met Office model acts to decrease the PV of air, which is then advected out of the boundary layer.

Chagnon *et al.* (2013) have also shown that the maximum in long-wave cooling at tropopause level, associated with the drop in humidity there, results in a diabatic PV dipole straddling the tropopause. Cooling gives a downwards diabatic mass transport across the tropopause, concentrating PV substance above and diluting PV substance below in the upper troposphere. Below the tropopause, in addition to the negative diabatic PV contribution associated with long-wave cooling, Chagnon *et al.* (2013) showed similar negative contributions to diabatic PV tracers resulting from the parametrized heating in the convection, microphysics and boundary-layer schemes. The time of integration of PV tracers, or equivalently the length of back trajectories from the outflow volume, is important to the diabatic PV deduced. For example, consider Figure 1. Define the PV minimum at 0900 UTC on the second day to be the time of 'outflow'. Then it is clear that the net PV change would be negative if calculated from any time after 0000 UTC on the first day. However, if the CET were followed back a further 6 h, the net PV change deduced would be positive. The negative contribution seen in diabatic PV tracers associated with latent heating (convection or microphysics schemes) reflects the fact that some air originated at different positions along the WCB where the average PV is higher and therefore there is a net decrease travelling with the CET to the outflow. It is worth noting that the trajectories in Martinez-Alvarado *et al.* (2013) are traced back to much nearer the ocean surface than in Pomroy and Thorpe (2000) or Joos and Wernli (2012), suggesting that the inflow volume associated with the CET in Martinez-Alvarado *et al.* (2013) extends below the boundary-layer cloud heating and is therefore more consistent with the assumptions about the inflow volume of the theory. This likely explains the net PV increase seen by Martinez-Alvarado *et al.* (2013), as opposed to the net PV decrease following the CET in the other two studies.

Rodwell *et al.* (2013) have shown that the worst forecast busts over Europe are associated with a distinctive situation six days beforehand, with an extended trough over the Rockies, moist southerly flow over the Eastern USA and the presence of mesoscale convective systems with active diabatic processes. They show that the diabatic PV tendency acts to slow down the eastwards progression of the Rossby wave and speculate that errors and uncertainties associated with unresolved diabatic processes in mesoscale convective systems may act to magnify initial-condition error or uncertainty in the subsequent forecast. Similarly, Chagnon *et al.* (2013) have shown that the PV dipole spanning the tropopause, produced systematically by diabatic processes, acts in the sense to enhance Rossby-wave propagation against the westerly flow (see their figure 10). The arguments presented here make it clear that any direct diabatic influence on Rossby waves at tropopause level must come through diabatic mass transfer from above or below. Also, net diabatic processes will influence the vertical location and extent of WCB outflow in isentropic coordinates. If the outflow is higher, it is likely to be characterized by a greater negative PV anomaly relative to its surroundings, even if the net diabatic modification of PV following a WCB is small.

Indirect diabatic effects are also important, where diabatically modified PV anomalies elsewhere have an influence at the tropopause via the anomalous horizontal winds that they induce. Davies and Didone (2013) have shown that forecast errors in the wind are expected to result in Rossby-wave-like propagation of errors. Furthermore, in their case study the phasing between the wind errors associated with PV at tropopause level and θ at 850 hPa was in the correct sense (see their figure 8) to result in mutual growth of errors at both levels by the baroclinic growth mechanism (Heifetz *et al.*, 2004), but mutual decay of the upper- and lower-level Rossby waves. Therefore, misrepresentation of diabatic processes giving rise to errors that underestimate low-level θ anomalies, or the outflow level for diabatic mass transport, can be expected to amplify errors elsewhere that act in the sense to reduce baroclinic Rossby-wave amplitude. The shape of the PV anomaly of the WCB outflow and its position relative to other tropopause-level features is important to the flow it 'induces' and its consequences for downstream evolution.

Acknowledgements

This study was motivated by experiments conducted as part of the DIAMET project, funded by the Natural Environment Research Council (grant NE/I005196/1). Particular thanks to Oscar Martinez-Alvarado for producing Figure 1. Thanks to the other collaborators in DIAMET for useful discussions, especially Jeffrey Chagnon, Mark Rodwell and Heini Wernli. The author thanks Michael McIntyre and an anonymous reviewer, whose careful comments resulted in considerable improvement of the article.

References

Agustí-Panareda A, Gray S, Methven J. 2005. Numerical modelling study of boundary-layer ventilation by a cold front over Europe. *J. Geophys. Res.* **110**: D18304, doi: 10.1029/2004JD005555.

Browning K. 1971. Radar measurements of air motion near fronts. *Weather* **26**: 320–340.

Browning K, Roberts N. 1994. Structure of a frontal cyclone. *Q. J. R. Meteorol. Soc.* **120**: 1535–1557.

Chagnon J, Gray S, Methven J. 2013. Diabatic processes modifying PV in a North Atlantic cyclone. *Q. J. R. Meteorol. Soc.* **139**: 1270–1282.

Davies H, Didone M. 2013. Diagnosis and dynamics of forecast error growth. *Mon. Weather Rev.* **141**: 2483–2501.

Harrold T. 1973. Mechanisms influencing the distribution of precipitation within baroclinic disturbances. *Q. J. R. Meteorol. Soc.* **99**: 232–251.

Haynes P, McIntyre M. 1987. On the evolution of vorticity and PV in the presence of diabatic heating and frictional or other forces. *J. Atmos. Sci.* **44**: 828–841.

Haynes P, McIntyre M. 1990. On the conservation and impermeability theorems for PV. *J. Atmos. Sci.* **47**: 2021–2031.

Heifetz E, Bishop C, Hoskins B, Methven J. 2004. The counter-propagating Rossby wave perspective on baroclinic instability. Part I: Mathematical basis. *Q. J. R. Meteorol. Soc.* **130**: 211–231.

Hoskins B. 1991. Towards a PV–θ view of the general circulation. *Tellus* **43AB**: 27–35.

Joos H, Wernli H. 2012. Influence of microphysical processes on the potential vorticity development in a warm conveyor belt: a case-study with the limited-area model COSMO. *Q. J. R. Meteorol. Soc.* **138**: 407–418.

Madonna E, Wernli H, Joos H, Martius O. 2014. Warm conveyor belts in the ERA-Interim dataset (1979–2010). Part I: Climatology and potential vorticity evolution. *J. Clim.* **27**: 3–26.

Martínez-Alvarado O, Joos H, Chagnon J, Boettcher M, Gray S, Plant R, Methven J, Wernli H. 2013. The dichotomous structure of the warm conveyor belt. *Q. J. R. Meteorol. Soc.*, doi: 10.1002/qj.2276.

Methven J, Hoskins B. 1999. The advection of high resolution tracers by low resolution winds. *J. Atmos. Sci.* **56**: 3262–3285.

Methven J, Arnold S, O'Connor F, Barjat H, Dewey K, Kent J, Brough N. 2003. Estimating photochemically produced ozone throughout a domain using flight data and a Lagrangian model. *J. Geophys. Res.* **108**: 4271, doi: 10.1029/2002JD002955.

Pomroy H, Thorpe A. 2000. The evolution and dynamical role of reduced upper-tropospheric PV in IOP1 of FASTEX. *Mon. Weather Rev.* **128**: 1817–1834.

Rodwell M, Magnusson L, Bauer P, Bechtold P, Bonavita M, Cardinali C, Diamantakis M, Earnshaw P, Garcia-Mendez A, Isaksen L, Kallen E, Klocke D, Lopez P, McNally T, Persson A, Prates F, Wedi N. 2013. Characteristics of occasional poor medium-range weather forecasts for Europe. *Bull. Am. Meteorol. Soc.* **94**: 1393–1405.

Thorncroft C, Hoskins B, McIntyre M. 1993. Two paradigms of baroclinic wave life cycle behaviour. *Q. J. R. Meteorol. Soc.* **119**: 17–55.

Wernli H, Davies H. 1997. A Lagrangian based analysis of extratropical cyclones. I: The method and some applications. *Q. J. R. Meteorol. Soc.* **123**: 467–489.